Iranian Journal of Science & Technology, Transaction A, Vol. 29, No. A1
Printed in The Islamic Republic of Iran, 2005

CHARACTERIZATION OF MERCAPTOBENZIMIDAZOLE ADSORPTION ON AN Au(111) ELECTRODE*

M. G. HOSSEINI [1**], T. SHAHRABI [2] AND R. J. NICHOLS [3]

[1] Electrochemistry Laboratory Research, Department of Physical Chemistry, Faculty of Chemistry, Tabriz University, I. R. of Iran, mg-hosseini@tabrizu.ac.ir
[2] Department of Materials Science, Faculty of Engineering, Tarbiat Modarres University, Tehran, I. R. of Iran
[3] Department of Chemistry, University of Liverpool, Crown Street, Liverpool, L69 7ZD, England

Abstract – The adsorption of 2-mercaptobenzimidazole (2-MBI) on Au(111) has been studied with cyclic voltammetry (CV), in-situ subtractively normalised interfacial FT-IR spectroscopy (SNIFTIRS) and scanning tunnelling microscopy (STM). Although adsorbed 2-MBI reduces the interfacial capacity and quenches the characteristic features of the cyclic voltammogram for sulfate adsorption, heterogeneous electron transfer to both the $[Fe(CN)_6]^{4-/3-}$ and $[Ru(NH_3)_6]^{3+/2+}$ redox systems is only partially impeded. Cyclic voltammetry has also been used to examine the reductive desorption of the thiolate in KOH electrolytes and its subsequent re-adsorption. From the reductive desorption charge, coverage of 2-MBI of 2.6×10^{-10} molecule cm^{-2} is estimated and this points to a flat-lying configuration of the monolayer, in agreement with a previous XPS study. The SNIFTIRS and electrochemical results show that adsorbed 2-MBI is displaced from the surface at positive potentials. STM imaging of adsorbed 2-MBI is also consistent with flat-lying molecules aligned in parallel rows.

Keywords – In-sutu iInfrared spectroscopic, scanning tunneling microscopy, Au(111), 2-mercaptobenzimidazole, 2-MBI, cyclic voltanmmetry

1. INTRODUCTION

Due to the electrochemical and bio-electrochemical importance of thin organic films, interest in their orientation and bonding to electrode surfaces has risen enormously in recent years. The last decade has seen the increasing application of techniques such as infrared spectroscopy and scanning tunnelling microscopy, which have helped in the formulation of detailed molecular level models, particularly for coherently organised monolayer assemblies. This is exemplified by the case of n-alkanethiols, where a comprehensive collection of data has been accumulated for the adsorption and electrochemical behaviour, particularly on gold substrates [1-6]. In contrast to alkanethiols, molecular level information regarding the adsorption of heteroaromatic thiols is scarce. However, there are notable recent studies that have provided detailed molecular level insights into the heteroaromatic thiolate adsorbates [1, 7-9].

Heterocyclic compounds containing sulphur and nitrogen atoms are well-known as effective surface-active compounds. They are widely used as anti-corrosion and anti-wear agents, metal plating bath additives and self-assembling monolayers, where they find application as promoting layers for electron transfer to redox metalloproteins [10-16]. We characterize here on the adsorption of 2-mercaptobenzimidazole (2-MBI) on Au(111). 2-MBI is employed as an effective inhibitor of copper

*Received by the editor January 13, 2004 and in final revised form December 25, 2004
**Corresponding author

corrosion [11-13]. It is also a well-known analytical reagent for mercury, and monolayers of 2-MBI on gold have been used for the electroanalytical determination of Hg (II) [17].

There is some disagreement in the literature about the molecular arrangement and bonding of 2-MBI onto gold electrode surfaces. This disagreement is understandable given the wide variety of conceivable bonding interactions between this molecule and a gold substrate. 2-MBI is known to exist in two tautomeric forms, the thioketo and thiole forms shown in Fig. 1. The thioketo form predominates in acidic and ethanolic solutions, while the thiolate form exists in sufficiently alkaline electrolytes. Some groups favour thiolate adsorption with the molecular plane perpendicular or off normal to the surface, with the monomolecular layers being described as "self assembling monolayers" [17]. The main driving forces for the adsorption in this configuration would be the formation of the gold-thiolate bond and possibly pi-stacking of the heteroaromatic rings, if they are suitably aligned. The other proposed configuration, with the adsorbate flat lying with respect to the substrate, involves a more multifarious interaction with the possibility of the heteroaromatic rings and imidazole groups also participating more directly in the surface bonding alongside the thiol. Xue et al. favour initial adsorption in the upright orientation followed by reorientation to form the flat lying adsorbate after warming the sample in air [14]. Berchmans et al. proposed an upright "self-assembly" of 2-MBI on gold, which is subsequently used to coordinate Hg(II) for stripping voltammetry determination [17]. On the other hand, Whelan et al. have characterised the adsorbed monolayer on Au(111) using XPS and conclude from the packing density and layer thickness estimation that 2-MBI adopts a flat-lying orientation [1]. These previous studies are complemented here by the voltammetric analysis of the behaviour of adsorbed 2-MBI, scanning tunnelling microscopy determination of the adsorbed monolayer and in-situ infrared spectroscopy.

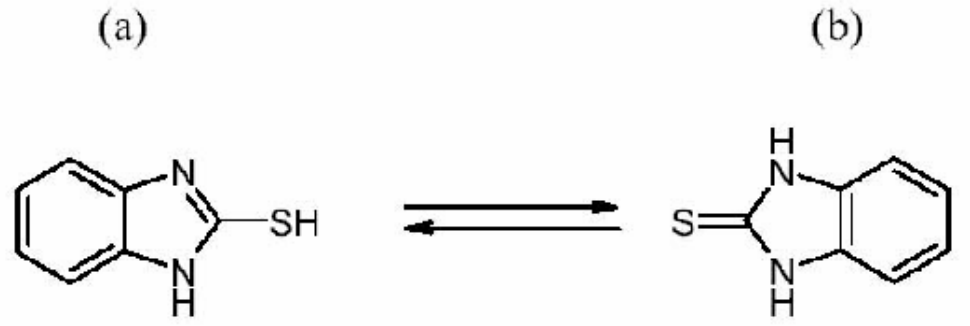

Fig. 1. The thiol (a) and thioketo (b) forms of 2-MBI

2. EXPERIMENTAL

a) 2.1 Solutions and Cyclic Voltammetry

The solutions were prepared with 2-mercaptobenzimidazole (2-MBI) from Arcos, analytical grade, potassium ferrocyanide (Analar, BDH), hexaammineruthenium(111) trichloride,(Alfa 99.9%), potassium dihydrogen phophate (Aristar BDH), dipotassium hydrogen phophate (Aristar BDH), potassium hydroxide (Aristar BDH), sulphuric acid (98%, Aristar BDH) and Milli-Q water (Millipore). All experiments were carried out at room temperature. An Autolab potentiostat was used for cyclic voltammetry. A standard calomel electrode (SCE) reference electrode was employed for the

electrochemical measurements, and all electrode potentials quoted in this manuscript are against this scale.

b) Substrates and Monolayer Formation

The Au(111) disc electrode (Metal Crystals and Oxides Ltd., Cambridge), 10 mm in diameter and 2 mm thick was used for the in-situ IR spectroscopy and CV experiments. This Au(111) electrode was prepared by polishing with successive grades of alumina powder down to 0.05 μm followed by electropolishing. Immediately prior to each experiment, this electrode was flame annealed in a Bunsen burner, left to cool for about 1 minute and then rinsed in Millipore water (Milli-Q). Monolayers of 2-MBI were formed by immersing the clean Au(111) electrode for 10-30 minutes in deoxygenated aqueous solutions containing 1mM of 2-MBI.

c) Infrared Spectroscopy

In-situ FTIR spectroscopy has been used here to monitor the adsorption as a function of potential. Potential difference infrared spectra were obtained using the subtractively normalised interfacial Fourier transform spectroscopy technique (SNIFTIRS). A three-electrode cell with a CaF_2 window (spectral cut-off below 1000 cm^{-1}) was employed for all spectroscopic experiments. The design of the cell is made in accordance with R. Nichol's method [18]. After preparation, the Au(111) electrode was aligned against the IR window. The thin layer cell formed usually has a thickness in order of between a few microns to several tens of microns. The potential was controlled with a potentiostat and waveform generator (Hi-Tek; England. DT 2101 and PPR1); the potential was switched between two pre-set potentials and *n* IR reflectance spectra collected at each potential. This procedure was repeated m times until a total number of *n* x *m* interfrograms were acquired for each of the two potentials. Typical values of *n* and *m* employed in this study were $n = 100$ and $m = 10$.

Before spectral collection, the solutions were purged with nitrogen (oxygen free, BOC Ltd.). An FT-IR spectrometer with an evacuable bench (Bruker IFS 66/S) with a liquid nitrogen cooled mercury cadmium telluride (MCT) detector being used for all the SNIFTIRS experiments. Normalised spectra were obtained by subtracting two spectra (R_2-R_1) obtained for different potentials and dividing this difference by R_1. Thus, the normalised change in reflectance is given by:

$$\Delta R/R = (R_2-R_1) / R_1$$

Polarization modulation infrared reflection absorption spectroscopy (PM-IRRAS) is ideally suited for recording the spectra of thin films on reflective substrates [19]. In this study a Bruker IFS 66/S infrared spectrometer has been used to record PM-IRRAS spectra of relatively thick (bulk-like) films of 2-MBI formed on a gold substrate.

d) STM experimental

The STM imaging was carried out with a Nanoscope E (Digital Instruments, Santa Barbara, CA). Gold on glass substrates were produced by vacuum evaporation of 2 nm of chromium, followed by 200 nm of gold (Metallhandel Schroeer GmbH). Prior to measurement, the gold samples were flame-annealed to produce (111) terraces. All images were acquired in constant-current mode.

3. RESULTS AND DISCUSSION

I. Cyclic Voltammetry

a) The Influence of 2-MBI on specific anion adsorption on Au(111)

Figure 2a shows a cyclic voltammogram of Au(111) in 0.1 M H_2SO_4 covering the double-layer region. In agreement with previous reports, the broad peak at approximately 300-600 mV corresponds to the specific adsorption of sulfate anions on the (1x1) Au electrode surface [20-23] . Overlaid in Fig. 2 is the cyclic voltammetry of Au(111) in a solution of 0.1 M H_2SO_4 with 1mM 2-MBI (Fig. 2b). It is clear to see from the comparison with the voltammogram of Au(111) in 0.1 M H_2SO_4, that the voltammetric features related to sulfate adsorption are effectively quenched in the presence of a 2-MBI monolayer. As well as quenching these characteristic features, the double layer capacity is reduced in a broad potential range, clearly indicating the formation of a surface film of 2-MBI. This reduction of the double-layer capacity upon the introduction of 2-MBI in the electrolyte is also apparent in 1 M KCl solutions (not shown here), indicating that it inhibits anion adsorption on the Au(111) electrode. Whelan et al. have also shown that 2-MBI provides an effective barrier to copper underpotential deposition [7]. It is also clear that 2-MBI retards H_2 evolution, with the onset of the cathodic H_2 evolution current being shifted to negative values when compared to clean Au(111) in sulphuric acid.

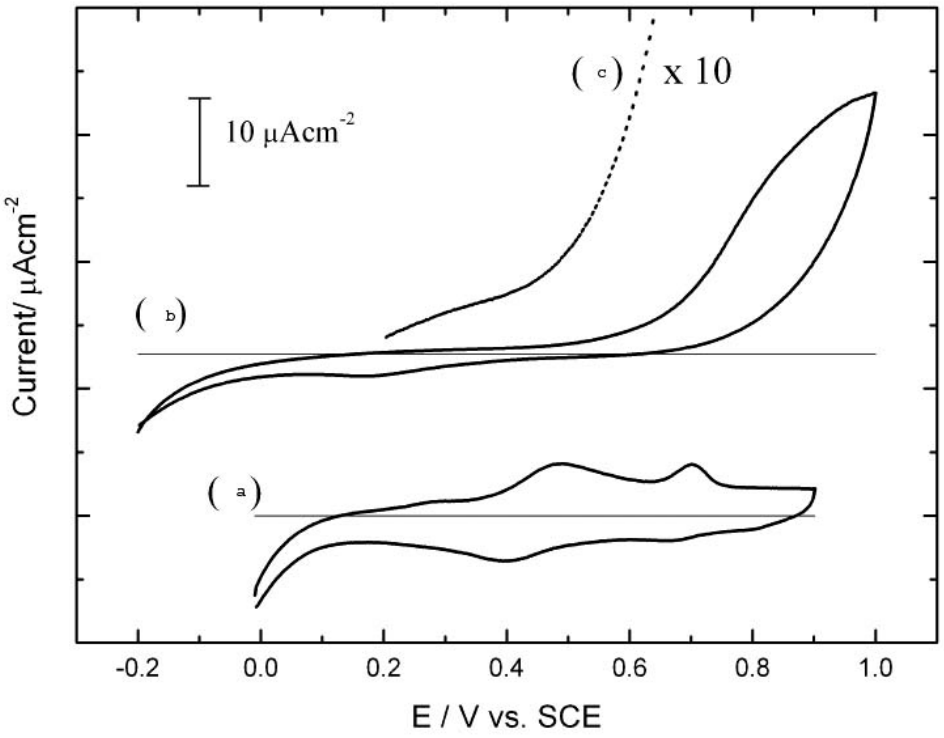

Fig. 2. Cyclic voltammograms for Au(111) in a) 0.1 M sulphuric acid, b) 0.1M sulphuric acid + 1mM 2-MBI. Scan rate = 50 mVs^{-1}. c) is a 10x enlargement of part of the anodic wave of b)

At more positive electrode potentials, an anodic wave is observed in Fig. 2b, which is presumably due to desorption of 2-MBI from the surface and concomitant oxidation. A previous voltammetric study has identified the oxidation of 1mM 2-MBI at around 300 -400 mV [24]. The onset of the anodic current can be more clearly seen in curve (c), which is a 10x magnification of the anodic wave of curve (b). This demonstrates that the onset of the anodic current is between about 200-400 mV.

b) The Influence of 2-MBI on the Redox Electrochemistry of the Ferro-/ Ferricyanide and Hexaammineruthenium (111) trichloride Systems

Further cyclic voltammetry experiments have been performed to assess the effect of 2-MBI surface films on electron transfer from the Au surface to redox couples in solution. Figs. 3a and 3b show cyclic voltammograms for the ferro-/ ferricyanide redox system obtained on Au(111) without and with 2-MBI, respectively. Even in the presence of 2-MBI the voltammetric peaks for this redox system are observed. This Figure indicates that 2-MBI does not form an effective barrier to heterogeneous electron transfer to this redox system, or that partial or complete 2-MBI desorption occurs by the electrode potentials characterising the ferro-/ ferricyanide redox system. Similar behaviour has been reported in a previous study for 2-mercaptobenzothiazole (2-MBT), which is structurally related to 2-MBI [25].

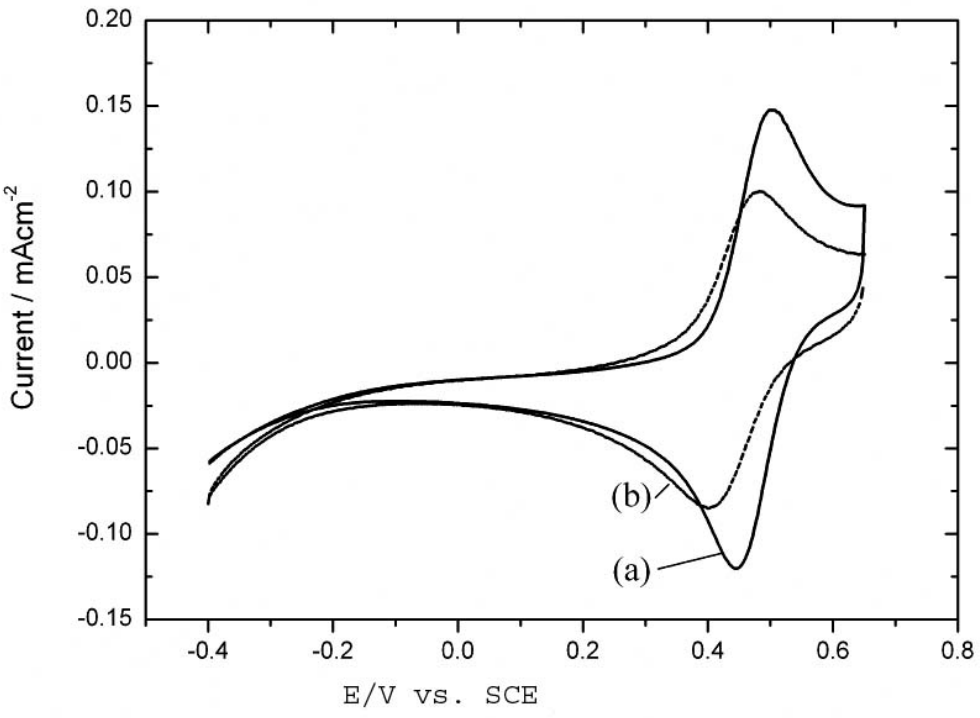

Fig. 3. Cyclic voltammograms on Au(111) a) 1 M H_2SO_4 + 1 mM Fe $(CN)_6^{4-/3-}$ redox system, b) 1 M H_2SO_4 + 1 mM Fe $(CN)_6^{4-/3-}$ redox system + 1 mM 2-MBI. Scan rate=50 mVs^{-1}

Since the redox wave for the ferro-/ ferricyanide couple occurs at rather positive potentials, where there are indications from the voltammetry in Fig. 2 that 2-MBI is displaced from the surface, complementary experiments have been performed with the $[Ru(NH_3)_6]^{3+/2+}$ redox system, which has a much more negative standard electrode potential. Figures 4a and 4b show two overlaid voltammograms for the redox electrochemistry of $[Ru(NH_3)_6]^{3+/2+}$, and for clean and 2-MBI covered

Au(111), respectively. These indicate that electron transfer to this redox couple occurs, even in the presence of the 2-MBI adsorbate.

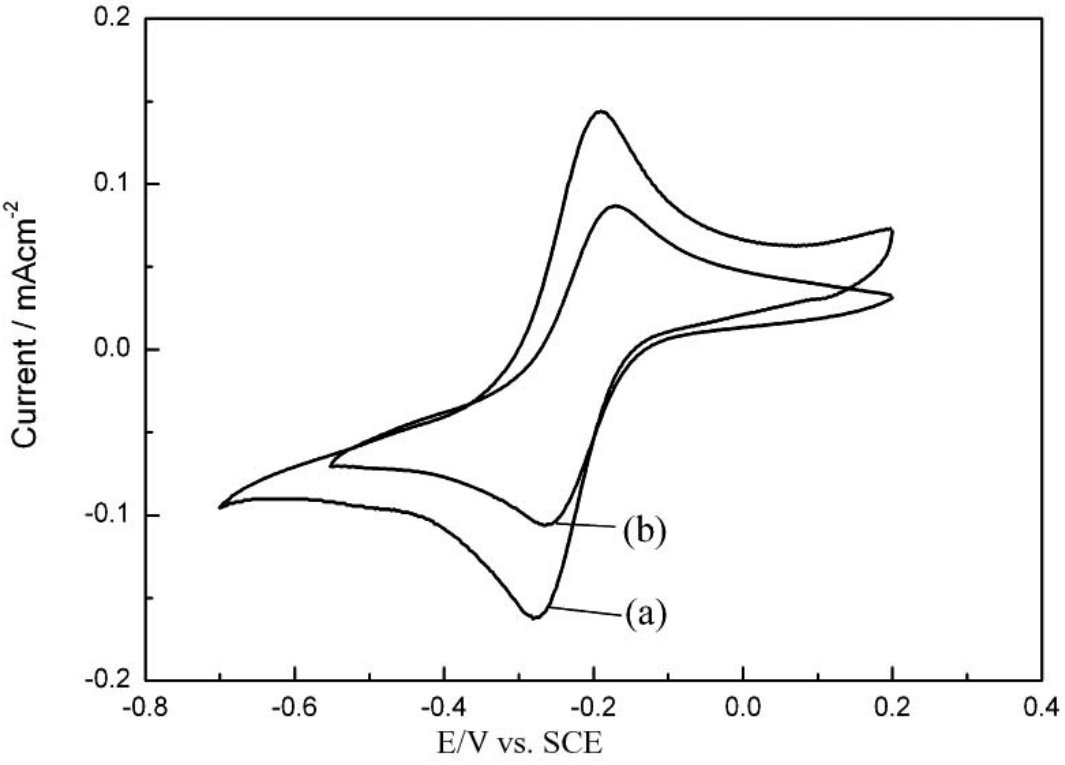

Fig. 4. Cyclic voltammograms of Au(111) in a) 1mM $[Ru(NH_3)_6]^{3+/2+}$ in 0.1 M pH=7 phosphate buffer solution, b) 1mM $[Ru(NH_3)_6]^{3+/2+}$ + 1 mM 2-MBI. Recorded in 0.1 M pH 7 phosphate buffer solution at a scan rate of 50 mVs^{-1}

c) Reductive desorption of the 2-MBI monolayers on Au(111)

Reductive desorption of thiolate monolayers on Au in a basic solution was first reported by Porter and co-workers [26-28], and this method has been widely applied to many thiolate systems by generally assuming the following one-electron process:

$$RSAu + e^- \longrightarrow RS^- + Au$$

In order to evaluate the surface concentration of 2-MBI monolayers, we have examined the voltammetry for the reductive desorption of the 2-MBI monolayer on Au(111) in 0.1 M KOH solution. A typical cyclic voltammogram for the reductive desorption of 2-MBI is shown in Fig. 5. Note that the reduction desorption of 2-MBI is quite different from that generally observed for thiols. Alkane thiols have limited solubility in aqueous electrolytes and the reductive desorption is generally obtained in the absence of thiolate in solution. However, the present voltammetry was conducted in electrolytes containing 2-MBI in solution. Therefore, in this case the reductive desorption in the cathodic scan is accompanied by adsorption of the thiolate in the anodic scan.

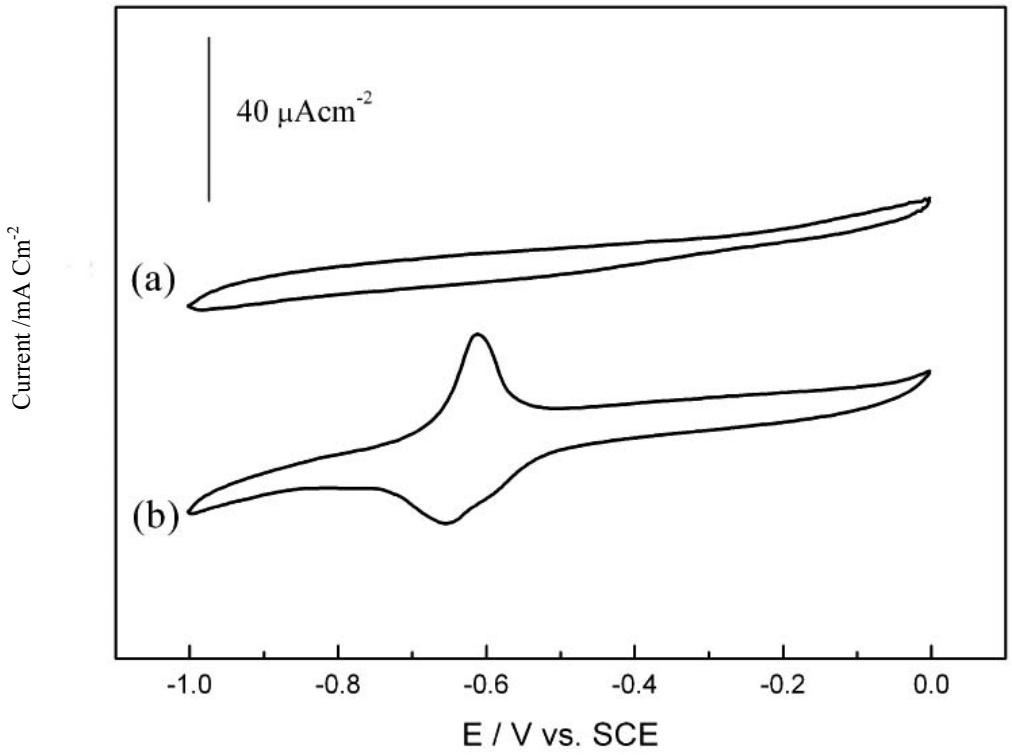

Fig. 5. Cyclic voltammograms for the reductive desorption of 2-MBI from Au(111) in a) 0.1 M KOH and b) 0.1 M KOH + 1 mM 2-MBI at scan rate of 50 mVs^{-1}

The cathodic peak for reductive desorption is very broad, with a full width at a half height (FWHH) of about 120 mV. Similarly, broad reductive desorption peaks have been observed for 2-mercaptopyridine (2-PySH) on Au(111) [9]. This was explained as arising from a relatively complicated desorption process of 2-PySH, not only involving bond breaking between sulphur and gold, but also involving the nitrogen position of the pyridine group [9]. In an analogous manner, we also take the broad desorption peak of 2-MBI as an indication of an adsorption geometry that does not solely involve surface coordination of the molecule through sulphur. This point will be discussed later in relation to the bonding model.

From the desorption branch of the voltammogram in Fig. 5, the charge consumed for reductive desorption can be estimated, which can then be used to estimate the surface concentration of the adsorbate ($q = nF\Gamma$, where Γ is the surface excess). The charge for reductive desorption of 2-MBI is estimated as 25 μCcm^{-2}. This corresponds to a surface coverage of 2.6×10^{-10} molecule cm^{-2}. Whelan et al.[1] have estimated the surface coverage for flat-lying and upright 2-MBI as 2.8×10^{-10} and 4.8×10^{-10} molecule cm^{-2}, respectively. Our measured surface coverage from the reductive desorption of 2.6×10^{-10} molecule cm^{-2} clearly favours the flat-lying model. This inference of a flat-lying adsorbate is used as a basis for interpreting the STM images, as discussed later in the text.

II. Infrared Spectroscopy

a) Infrared Spectra of Bulk 2-MBI

Before discussing the in-situ infrared spectra obtained in the spectro-electrochemical cell, the IR spectra of bulk 2-MBI will be discussed. No definitive IR spectroscopic study of 2-MBI could be

found in the literature, so the spectra have been recorded and then assigned with the aid of density functional calculations (DFT). We found that the best quality of IR spectra of bulk 2-MBI could be obtained using polarization modulation infrared reflection absorption spectroscopy (PM-IRRAS). A droplet of a saturated ethanolic solution of 2-MBI was placed on a gold-coated glass slide and allowed to dry to form a thick film of bulk 2-MBI. The resulting PM-IRRAS spectrum is shown in Fig. 6. The bands observed are shown in Table 1, together with results of DFT calculation for 2-MBI. Density functional calculations (SVWN/DN*) were performed using Spartan Pro™. These DFT calculations show that vibrations in the region of 1000-1700 cm^{-1} arise from multifarious combinations of RC-H bends in plane stretches and deformations of both rings, RS-H bends and RN-H bends. Most of the vibrations shown in Table 1 are complex combination modes, and as such it has not been possible to definitively assign the spectra. However, most importantly DFT calculations show that these modes are overwhelmingly in plane with little significant out of plane motion. This is important for the subsequent evaluation of the SNIFTIRS spectra for 2-MBI adsorption.

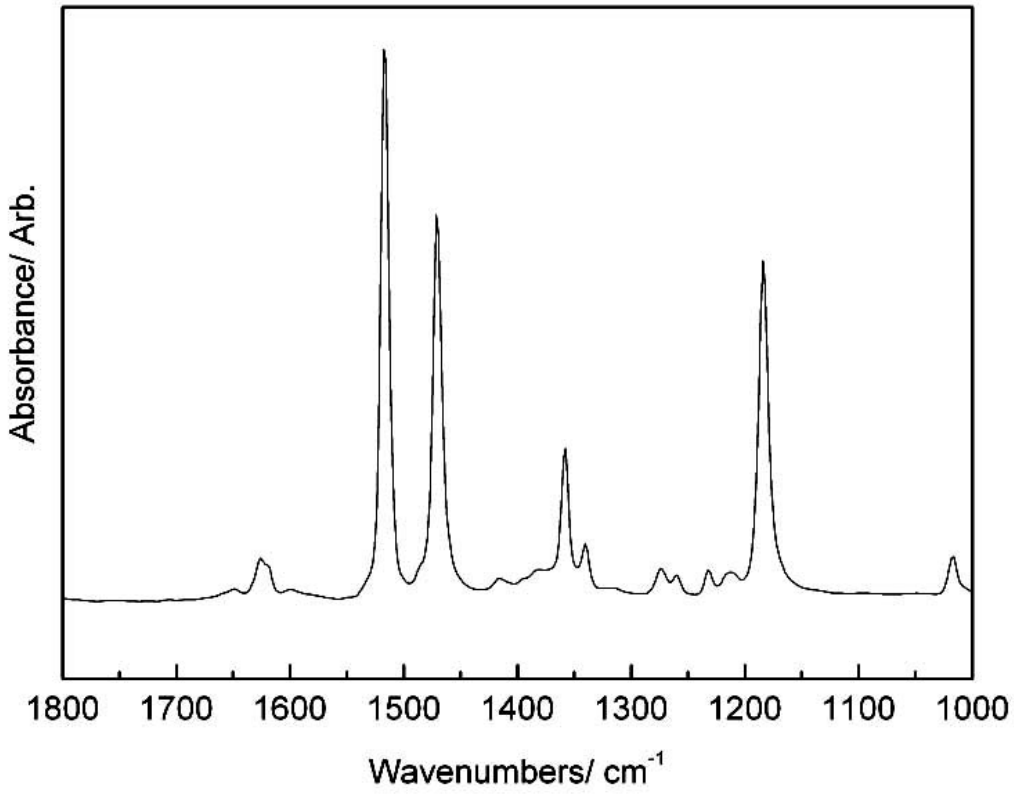

Fig. 6. A PM-IRRAS of bulk 2-MBI

Table 1. Band positions/ cm^{-1} and possible assignments for 2-mercaptobenzimidazole (2-MBI)

Band/ cm^{-1} and Strength	DFT calculation	Assignment of DFT Result
1017 w	1018	C-H def. and in plane ring def.
	1108	C-H def. and in plane ring def.
	1141	C-H bend, RN-H def. and in plane ring def.
1184 s	1158	RN-H def., RS-H def., C-H def. and ring def.
	1231	C-H def. and in plane ring def.
	1296	In plane ring def., C-H def. and C-S-H def.
1358 m	1379	RN-H def., C-H def., in plane ring def., C-S-H def.
	1426	C-H def., in plane ring def. and RN-H def.
1470 s	1469	C-H def. and in plane ring def.
	1501	C-H def., in plane ring def. and RN-H def.
1516 s	1513	C-H def., RN-H def., in plane ring def. and C-S-H def.
	1618	C-H bend, in plane ring stretch. and RN-H def.
1652 s	1662	C-H def., in plane ring def. and RN-H def.

Key: w=weak, m=medium, s=strong, def.=deformation

b) In-situ subtractively normalised interfacial FT-IR spectroscopy (SNIFTIRS)

SNIFTIRS spectra have been recorded with E_2 being increased in a stepwise manner in the potential range of –200 to 600 mV. These SNIFTIRS spectra are in reference, with respect to spectra recorded at the base potential, E_1 = –300 mV. Selected normalized spectra are shown in Fig. 7. For potentials between –300 and 100 mV, no spectral features are observed. At 200 mV, several weak negative going bands appear in the spectral region between 1600 and 1000 cm^{-1}. These bands increase in intensity from E_2 = 200 mV to E_2 = 600 mV, with peak position at 1512, 1468, 1352, 1268 and 1172 cm^{-1}. Since these bands are pointing downwards, they correspond to increased spectral absorbance at E_2, i.e. at the positive potential limit.

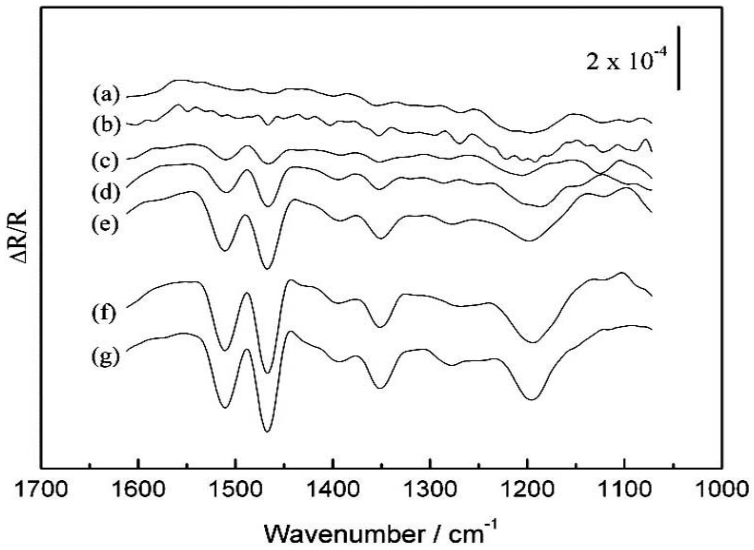

Fig. 7. SNIFTIRS spectra for Au(111) electrode in 0.1 M H_2SO_4 + 1 mM 2-MBI recorded with p-polarised light. For these spectra the reference potential, E_1 was set at – 300 mV, and E_2 was respectively set at 0 (a), 100 (b), 200 (c), 300 (d), 400 (e), 500 (f) and 600 (g) mV

To distinguish between adsorbed and solution free species, IR experiments with s- and p-polarised light have been performed. By application of the surface selection rule, bands corresponding to adsorbed species appear only in the spectra with p-polarized light, but not for s-polarized light, since the electric field of the s component vanishes at the metal surface. On the other hand, species dissolved in the thin layer may be detected with both polarization states. The comparison between s- and p- spectra is shown in Fig. 8. From this Fig., which is a SNIFTIRS difference spectrum, it is not possible to unequivocally determine whether positive going bands arising from the adsorbate are present due to the presence of large downwards pointing bands from desorbed 2-MBI. This demonstrates that all discernable bands presented in the p-polarised spectra also appear in the s-polarised spectra. A plot of the intensity of the 1468 cm^{-1} spectral band versus electrode potential is presented in Fig. 9. The significant increase in the band intensity at potentials greater than 300 mV indicates replacement or oxidation of 2-MBI.

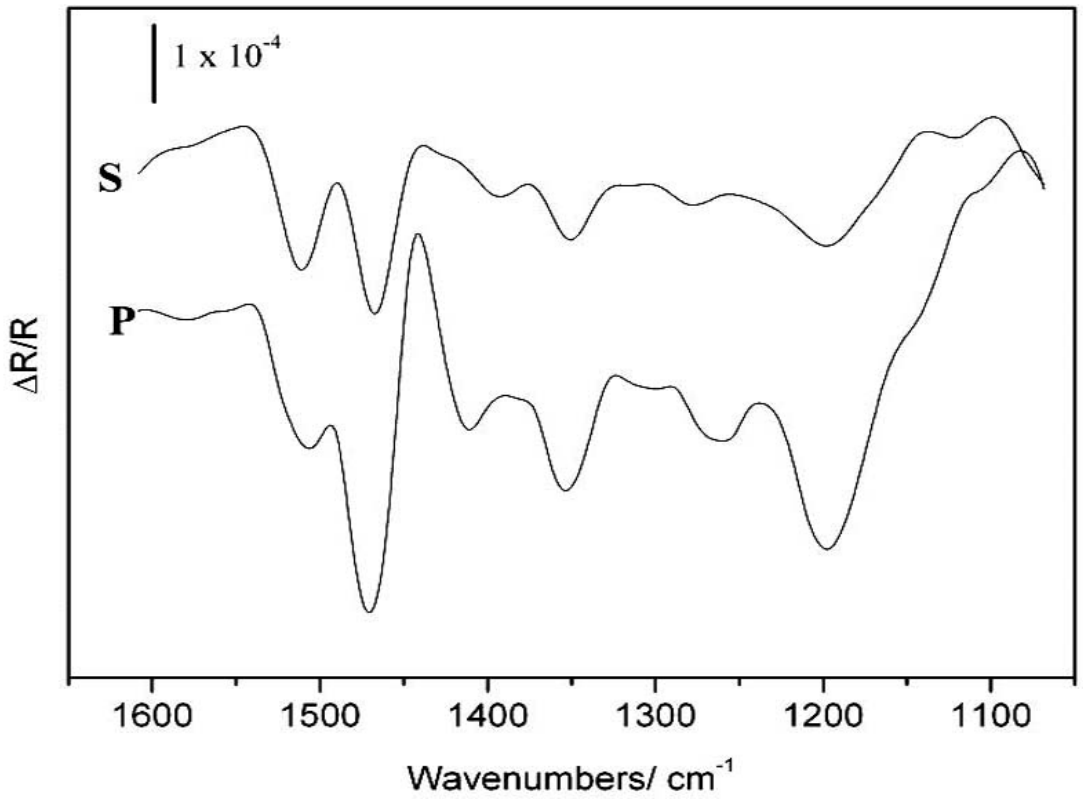

Fig. 8. Potential difference spectra for Au(111) in 0.1 M H_2SO_4+ 1 mM 2-MBI recorded at E_2= 400 mV with s- and p- polarised light, respectively

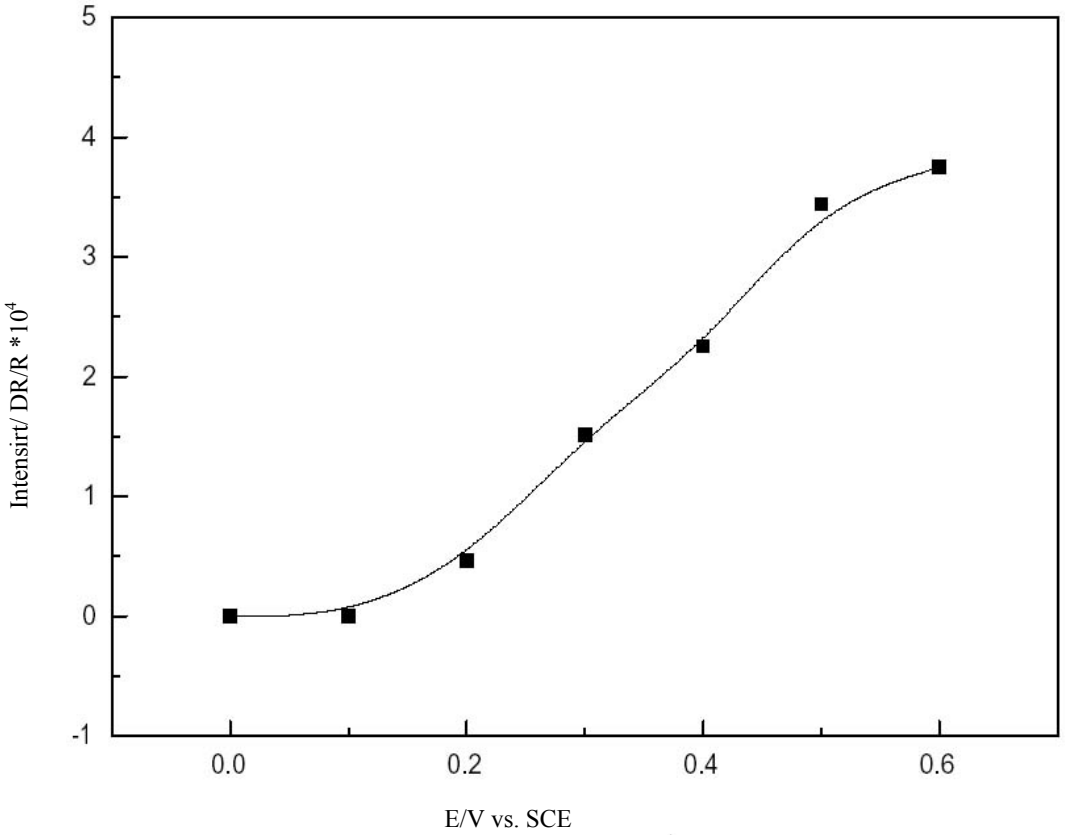

Fig. 9. Dependence of intensity the 1468 cm^{-1} SNIFTIRS band (C-H deformation and in plan ring deformation mode) on electrode potential, Recorded for Au(111) in 0.1 M H_2SO_4 + 1mM 2-MBI

We also note that there is an anodic current in the voltammogram for 2-MBI adsorbed on Au(111) when the electrode potential is extended beyond about 0.4 V (see Fig. 2). This anodic current is attributed to electro-oxidation of 2-MBI. Infrared spectra recorded at E > + 600 mV show that the major in-plane vibrational modes of 2-MBI between 1600-1000 cm^{-1} are preserved. This implies that the electrochemical oxidation leaves the heterocyclic ring intact and it is likely that it proceeds by oxidation of the thiol group. Thiol groups are known to be susceptible to oxidation to sulfonates so a possible half-reaction scheme would be:

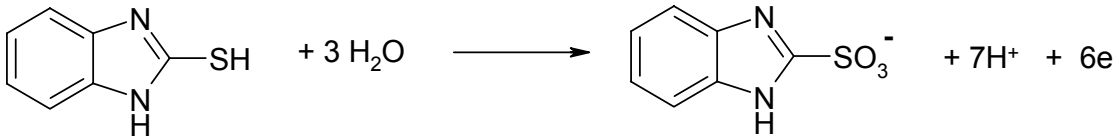

However, such a reaction scheme could not be verified spectroscopically, since in-plane vibrational modes of the heterocyclic ring are located at similar frequencies to S-O stretching modes.

III. Scanning Tunnelling Microscopy

Figure 10 shows an STM image of 2-MBI covered Au(111), imaged in air. Three lines are drawn on this image. Line X-Y is co-linear with a step edge on the Au(111) substrate. A large terrace lies above line X-Y, and is covered with an extended domain of adsorbed 2-MBI. This features a long-range corrugation parallel to line C-D and a shorter-range corrugation in the direction parallel to A-B. The respective periodicities are 6.1 and 1.5 nm. The larger corrugation is likely to arise from a Moiré pattern, which is caused by a mismatch between the substrate and adsorbate lattice. The observation of a complex Moiré pattern indicates that 2-MBI does not form a simple commensurate adlayer on the Au(111) substrate. The shorter-range corrugation is interpreted as arising from ordered parallel rows on adsorbed 2-MBI.

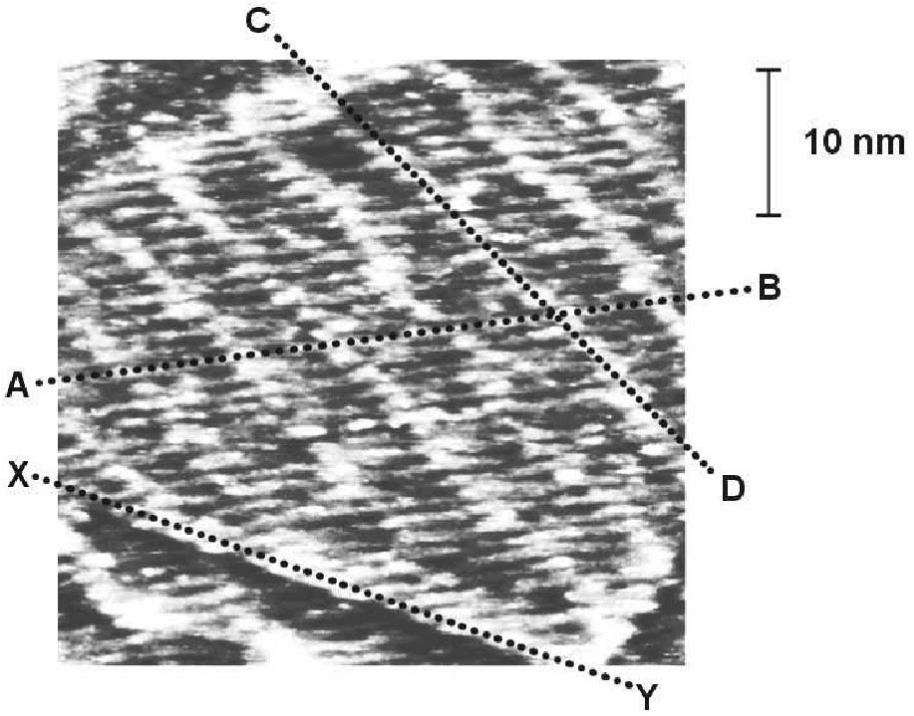

Fig. 10. An STM image of 2-MBI on Au(111) recorded in air with a tunnelling current of 0.3 nA, The ad-layer was formed by immersion for 10 minutes in ethanol containing 1mM 2-MBI

In interpreting the shorter-range parallel corrugation rows seen in the STM images, the structure of bulk crystalline 2-MBI has been referred to, in order to see if any structural similarities exist [29]. The crystal structure of 2-MBI has been determined as monoclinic with the $P2_1/m$ space group and unit cell dimensions of a = 4.933 Å, b = 8.594 Å, c = 8.343 Å, and $\beta = 91.71^{o}$. 2-MBI crystals form close packed sheets along the b-c plane. A representation of these sheets is shown in Fig. 11. The sulphur atoms are arranged along relatively well-packed rows with an up-down alternation, which increases the packing density of the non-coplanar sheets. The two adjacent horizontal rows of sulphur atoms shown in Fig. 11 are separated by 1.31 nm, but this spacing would be increased if the molecules were forced into a coplanar structure. Several STM studies have shown that sulphur within molecular adsorbates can give a high contrast [30]. Given this, the stripes seen in the STM image, which are separated by 1.5 ± 0.2 nm (Fig. 10) are strongly suggestive of adjacent rows of sulphur

atoms. The larger spacing in the STM image when compared to the b-c plane of crystalline 2-MBI could either arise from forcing the sheets of MBI molecules into a coplanar structure, or the sulphur atoms adjusting their site occupancy to higher coordination sites. A possible model has been proposed on the basis of a flat lying orientation, however the IR results cannot definitely rule out a tilted orientation for the adsorbate, and as such, this model is not unique. In the eventuality of a tilted orientation for 2-MBI, the STM image would require reinterpretation. In any case, a higher resolution would be required to unequivocally identify a unit cell. This flat lying orientation is in agreement with a previously reported XPS study and consistent with the coverage deduced from the reductive desorption experiments presented here [1].

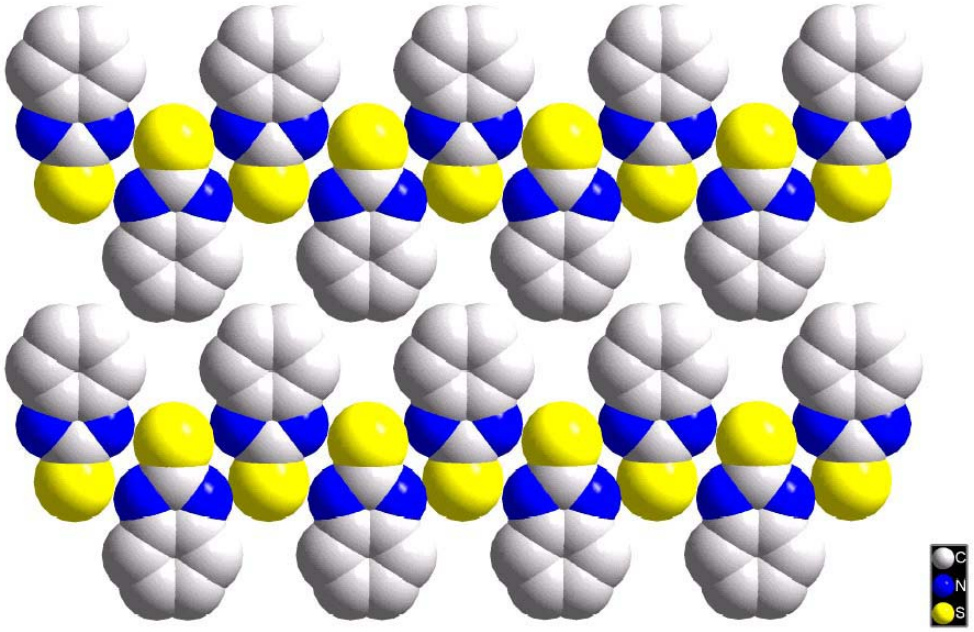

Fig. 11. A representation of the molecular arrangement in b-c plane of crystalline 2-MBI, This is a non-planar sheet with packing density being increasing by an up-down alternation between adjacent molecules that cannot be seen in this top-view representation

4. CONCLUTIONS

In summary, we have presented here a study of 2-MBI adsorption on Au(111) using cyclic voltammetry, in-situ infrared spectroscopy and ex-situ STM. On the basis of reductive desorption a coverage of about 2.6 x 10^{-10} molecule cm^{-2} is derived. This clearly supports a model for flat-lying 2-MBI, since the theoretical coverage of the flat-lying adsorbate is 2.8 x 10^{-10}, while that for the upright adsorbate is 4.8 x 10^{-10} molecule cm^{-2}. This flat-lying adsorbate reduces the double layer capacity of Au(111) and suppresses H_2 evolution. However, electron transfer to the $[Ru(NH_3)_6]^{3+/2+}$ redox system is not blocked by adsorbed 2-MBI. Cyclic voltammetry also shows that 2-MBI is adsorbed on Au(111) over a limited electrode potential with desorption and oxidation occurring for potentials greater than 200-400 mV.

The wavenumber range between 1000-1700 cm^{-1} has been examined, where a number of in-plane vibrational modes of 2-MBI appear. None of these vibrational modes are observed for the adsorbate, indicating that its molecular plane is parallel to the metal electrode. Spectral bands are only observed in the SNIFTIRS experiments when the potential is extended $\geq$ +200 mV. These spectral

bands correspond to 2-MBI that is desorbed from the surface into the thin layer spectro-electrochemical cell. Since there is a pronounced anodic current, which is particularly apparent for E > 0.6 V, it is concluded that desorption is accompanied by oxidation of 2-MBI. The vibrational bands observed for oxidatively desorbed 2-MBI are similar to 2-MBI, indicating that the heterocyclic ring of 2-MBI is preserved, even following electrochemical oxidation. This implies that electrooxidation involves the thiolate, which is probably oxidized to the sulfonate group. By comparison, alkane thiols adsorbed on gold are known to be susceptible to photooxidation to sulfonates, particularly in cases where atmospheric oxygen can penetrate to the Au surface [30]. Although the STM images are strongly suggestive of parallel rows of flat lying 2-MBI, the resolution of the image precludes the determination of an exact unit cell configuration.

Acknowledgments- This work was supported by a grant from the Ministry of Science, Research and Technology, Iran and by EPSRC (UK). The authors would like to thank Dr. Wolfgang Haiss for useful discussions.

REFERENCES

1. Whelan, C. M., Barnes, C. J., Brown, N. M. D. & Anderson, C. A. (1998). The influence of heterocyclic thiols on the electrodeposition of Cu on Au(111). *Applied Surface Science, 134*, 144.
2. Bain, C. D., Troughton, E. B., Tao, Y. T., Evall, J., Whitesides, G. M. & Nuzzo, R. G. (1989). Formation of monolayer films by the spontaneous assembly of organic thiols from solution onto gold. *Journal of the American Chemical Society*, *111*, 321.
3. Ulman, A. (1991). *An introduction to Ultra thin Organic Films: from Langmuir-Blodgett to self-Assembly*. New York, Academic Press.
4. Sawaguchi, T., Sato, Y. & Mizutani, F. (2001). In situ STM imaging of individual molecules in two-component self-assembled monolayers of 3-mercaptopropionic acid and 1-decanethiol on Au(111). *Journal of Electroanalytical Chemistry, 496*, 50.
5. Smith, E. A., Wanat, M. J., Cheng, Y. F., Barreira, S. V. P., Frutos, A. G. & Corn, R. M., Formation. (2001). Spectroscopic characterization, and application of Sulfhydryl-Terminated alkanethiol monolayers for the chemical attachment of DNA onto gold surfaces. *Langmuir*, *17*, 2502.
6. Clavilier, J., Evetlicic, V. & Zutic, V. (1995). Thionine self-assembly on polyoriented gold and sulphur-modified gold electrodes. *Journal of Electroanalytical Chemistry*, *386*, 157.
7. Whelan, C. M., Smyth, M. R. & Barnes, C. J. (1998). The influence of heterocyclic thiols on the electrodeposition of Cu on Au(111). *Journal of Electroanalytical Chemistry*, *441*,109.
8. Yoshimoto, S., Sawaguchi, T., Mizutani, F. & Taniguchi, I. (2000). Voltammetric curves for Au (111) in acid media: A comparison with Pt (111) surfaces. *Electrochemistry Communications*, *2*, 39.
9. Sawaguchi, T., Mizutani, F., Yoshimoto, S. & Taniguchi, I. (2000). The adsorption of sulfate on gold (111) in acidic aqueous media: adlayer structural inferences from infrared spectroscopy and scanning tunnelling microscope. *Electrochimical Acta, 45*, 2861.
10. Dafali, B. H. A., Aounity, A., Mokhlisse-Kertti, R. S. & Elkachemi K. (2000). 2-Mercapto-1-methylimidazole as corrosion inhibitor of copper in aerated 3% NaCl solution. *Annal. Chemical. Science, Materials, 25*, 437.
11. Subramanian, R. & Lakshminarayanan, V. (2002). Effect of adsorption of some azoles on copper passivation in alkaline. *Corrosion Science*, *44*, 535.

12. Xue, G. & Dai, Q. P. (1994). SERs and IR Studies of the reaction of an oxidized surface and etched surface of copper with 2-mercaptobenzimidazole. *Spectroscopy Letters*, *27*, 341.
13. Xue, G., Huang, X. Y., Dong, J. & Zhang, J. F. (1991). The formation of effective anti-corrosion solution film on copper surfaces from 2- mercaptobenzimidazole solution. *Journal of Electroanalytical Chemistry, 310*, 139.
14. Xue, G. & Lu, Y. (1994). Various Adsorption States of 2-Mercaptobenzimidazole on the Surfaces of Gold and Silver Studied by Surface Enhanced Raman Scattering. *Langmuir, 10*, 967.
15. Marconato, J. C., Bulhoes, L. O. & Temperini, M. L. (1998). A spectroelectrochemical study of the inhibition of the electrode process on copper by 2-mercaptobenzothiazole in ethanolic solutions. *Electrochimical Acta*, *43*, 771.
16. Zhang, J. Y., Liu, W. M. & Xue, Q. J. (1999). Effect of molecular structure of heterocyclic compounds containing N, O and S on their tribological performance. *Wear*., *231*, 65.
17. Berchmans, S., Arivukkodi, S. & Yegnaraman, V. (2000). Self-assembled monolayers of 2-mercaptobenzimidazole on Gold: Stripping voltammetric determination of Hg(II). *Electrochemistry Communications*, *2*, 226.
18. Chen, P. Y., Smith, M. J. & Garland, B. (2000). *American Laboratory*, *32*, 36.
19. Magnussen, O. M., Hagebock, J., Hotlos, J. & Behm, R. J. (1992). *Faraday Discussions*, *329*.
20. Scherson, D. A. & Kolb, D. M. (1984). Voltammetric curves for Au(111) in acid media: A comparison with Pt (111) surface, *Journal of Electroanalytical Chemistry*, *176*, 353.
21. Mrozek, P., Han, M., Sung, Y. E. & Wieckowski, A. (1994). Sulfate adsorption on a Au(111) electrode studied by AES, CEELS, LEED and cyclic voltammetry *Surface Science*, *319*, 21.
22. Edens, G. J., Gao, X. P. & Weaver, M. J. (1994). The adsorption of sulfate on gold (111) in acidic aqueous media: adlayer structural inferences from infrared spectroscopy and scanning tunneling microscope. *Journal of Electroanalytical Chemistry, 375*, 357.
23. Shahrokhian, S., Amini, M. K., Mohammadpoor-Baltork, I. & Tangestaninejad, S. (2000). Potentiometric Detection of 2-Mercaptobenzimidazole and 2-Mercaptobenzothiazole at Cobalt Phthalocyanine Modified Carbon-Paste Electrode. *Electroanalysis, 12*, 863.
24. Bharathi, S., Yegnaraman, V. & Rao, G. P. (1993). Potential-dependent "opening" and "closing" of self-assembled 2-mercaptobenzthiazole on gold substrates. *Langmuir, 9*, 1614.
25. Lamp, B. D., Hobara, D., Porter, M. D., Niki, K. & Cotton, T. M. (1997). Correlation of the Structural Decomposition and Performance of Pyridinethiolate Surface Modifiers at Gold Electrodes for the Facilitation of Cytochrome *c* Heterogeneous Electron-Transfer Reactions. *Langmuir*, *13*, 736.
26. Widrig, C. A., Chung, C. & Porter, M. D. (1991). The electrochemical desorption of n-alkanethiol monolayers from polycrystalline Au and Ag electrodes. *Journal of Electroanalytical Chemistry*, *310*, 335.
27. Zhong, C. J. & Porter, M. D. (1994). Evidence for Carbon-Sulfur Bond Cleavage in Spontaneously Adsorbed Organosulfide-Based Monolayers at Gold. *Journal of the American chemical society*, *116*, 1616.
28. Ravikumar, K., Mohan, K. C., Bidyasagar, M. & Swamy, G. (1995). Crystal structure of 2-mercaptobenzimadozole and bis [2-mercaptobenzimidazole] dichlorocobalt (II)*, Journal of Chemical Crystallography*, *25*, 325.
29. Giancarlo, L., Cyr, D., Muyskens, K. & Flynn, G. W. (1998). Scanning Tunneling Microscopy of Molecular Adsorbates at the Liquid-Solid Interface: Functional Group Variations in Image Contrast. *Langmuir*, *14*, 1465.
30. Rieley, H., Kendall, G. K., Zemicael, F. W., Smith, T. L. & Yang**,** S. H. (1998). X-ray Studies of Self-Assembled Monolayers on Coinage Metals; Alignment and Photooxidation in 1, 8-Octanedithiol and 1-Octanethiol on Au. *Langmuir*, *14*, 5147.